CORROSION SCIENCE AND TECHNOLOGY, Vol.3, No.6(2004), pp.245~250

Effects of Cement Alkalinity on the Time-to-Corrosion of Reinforcing Steel in Concrete under Chloride Exposure

Jingak Nam, William H. Hartt, and Kijoon Kim*

Florida Atlantic University, Florida, USA
**Korea Maritime University, Busan, Korea*

A series of classical G109 type concrete specimens was exposed to cyclic wet and dry ponding with 15 w/o NaCl solution for approximately five years. Mix design variables included 1) three cement alkalinities (EqA of 0.97, 0.52, and 0.36) and 2) three water-cement ratios (0.50, 0.41, and 0.37). To determine the corrosion initiation time, corrosion potential and macro-cell current between top and bottom bars were monitored. Subsequent to corrosion initiation, specimens were autopsied and visually inspected. Concrete powder samples were collected from top rebar trace and chloride concentration was measured. Also, time-to-corrosion, T_i, for specimens of the individual mix designs was represented using Weibull analysis.

Time-to-corrosion was a distributed parameter; and because of this, corrosion initiation of four identical specimens for each mix varied, often over a relatively wide range. Specimens fabricated using the lowest water cement ratio and the highest alkalinity cement exhibited the longest time-to-corrosion initiation and the highest chloride threshold levels. Time-to-corrosion did not increase monotonically with cement alkalinity, however, presumably as a consequence of relatively high Cl^- binding in the lower pore water pH range. The chloride threshold level, Cl_{th}, increased with increasing T_i and, consequently, was greatest for the highest cement alkalinity specimens.

Keywords : *concrete, water cement ratio, cement alkalinity, reinforcing steel, time-to-corrosion, Weibull analysis*

1. Introduction

The fact that Portland cement concrete affords corrosion protection to embedded steel has been recognized for more than a century. The protective mechanism is mostly due to the thin passive film which is formed and maintained in the alkaline environment produced by cement hydration.[1] However, this passive film can become locally unstable and corrosion can initiate when chloride concentration at the steel surface achieves a critical concentration[2] or pH of the concrete pore water decreases (or both). As such, electrolyte composition is a dominant factor affecting the corrosion process with the most prevalent activator being chlorides and the passivator hydroxides. Consequently, time-to-corrosion, T_i, for concrete structures is determined by the competing influences of these species.[3]

Chloride can be introduced into concrete as a contaminant in the original mix, by exposure to de-icing salts, or from seawater (or a combination of these). Once in the concrete, chloride may exist as free ions or bound hydration products. Chloride concentration, $[Cl^-]$, at the steel depth is mainly determined by 1) composition of these species in the environment, 2) its ingress rate into the concrete, and 3) concrete cover over the steel.[4]

The pH of concrete pore solution is normally governed by the relatively small quantity of alkalis which exist in the cement clinker. With the advent of pore water expression[5)-7)] and theoretical considerations, it was recognized that K^+ and Na^+ are the predominant cations in concrete pore water. This happens because at the high pH generated by these species ($pH > 13$), the solubility of $Ca(OH)_2$ is relatively low.[8),9)] Due to the additional release of hydroxide ion from alkali, therefore, the pH in concrete pore water saturated with $Ca(OH)_2$ become about 13 to 13.5.[9)]

While it is generally recognized that the chloride threshold level, Cl^-_{th}, increase with increasing alkalinity, no systematic investigations that address this have been performed. Therefore, the objective of the present research was the evaluation of the effects of cement alkalinity for extending time-to-corrosion initiation by means of elevating Cl^-_{th}.

2. Experimental procedures

2.1 Materials

Cements of three alkalinities which are designated as "low alkalinity" (LA), "normal alkalinity" (NA), and "high" (HA) were employed in fabricating the concrete specimens. Table 1 lists the composition for each of these cements along with equivalent alkalinity (EqA), as determined from the equation,

$$EqA = w/o\ Na_2O + 0.658 \cdot w/o\ K_2O, \quad (1)$$

This revealed EqA values of 0.36 for LA cement, 0.52 for NA, and 0.97 for HA. These same designations were used to identify individual concrete specimens according to the cement type employed.

Table 1. Composition of three cement types and the equivalent alkalinity (EqA).

Compound	SiO_2	Al_2O_3	Fe_2O_3	Fe_2O_3	MgO	SO_3	Na_2O	K_2O	EqA
LA	21.93	5.16	3.7	65.02	1.39	2.38	0.099	0.39	0.36
NA	21.88	5.64	3.87	64.42	0.98	2.87	0.164	0.54	0.52
HA	20.63	4.44	2.56	63.39	3.85	3.96	0.192	1.19	0.97

2.2 Specimens

Fig. 1 schematically illustrates the design of the standard G109 type specimen.[10] Rebar ends were sealed at both ends with heat shrink tubing prior to concrete placement. Diameter of the reinforcement steel was 12.7 mm, and surface preparation involved wire brushing just prior to placement. The four sides were sealed with an epoxy coating with the bottom and top faces remaining bare. A plastic container was mounted on top of specimen for cyclic ponding. Concrete cover for the top and bottom bars was 25 mm. The top and bottom bars were electrically connected with a 100 Ω resistor to measure macro-cell current. Four specimens were fabricated for each mix design based upon selected combinations of cement alkalinity and water-cement ratio (w/c). Table 2 lists mix designs and specimen configurations.

2.3 Exposures and specimen analyses

A one-week wet and one-week dry ponding cycle con

Table 2. Specimen mix designs and designations.

Specimen	Alkalinity	w/c	Sand (kg/m^3)
LA0.37	Low	0.37	761
LA0.41		0.41	719
LA0.50		0.50	625
NA0.37	Normal	0.37	761
NA0.41		0.41	719
NA0.50		0.50	625
HA0.37	High	0.37	761
HA0.41		0.41	719
HA0.50		0.50	625

*Each mix had 400 kg/m^3 of cement and 1004 kg/m^3 of stone.

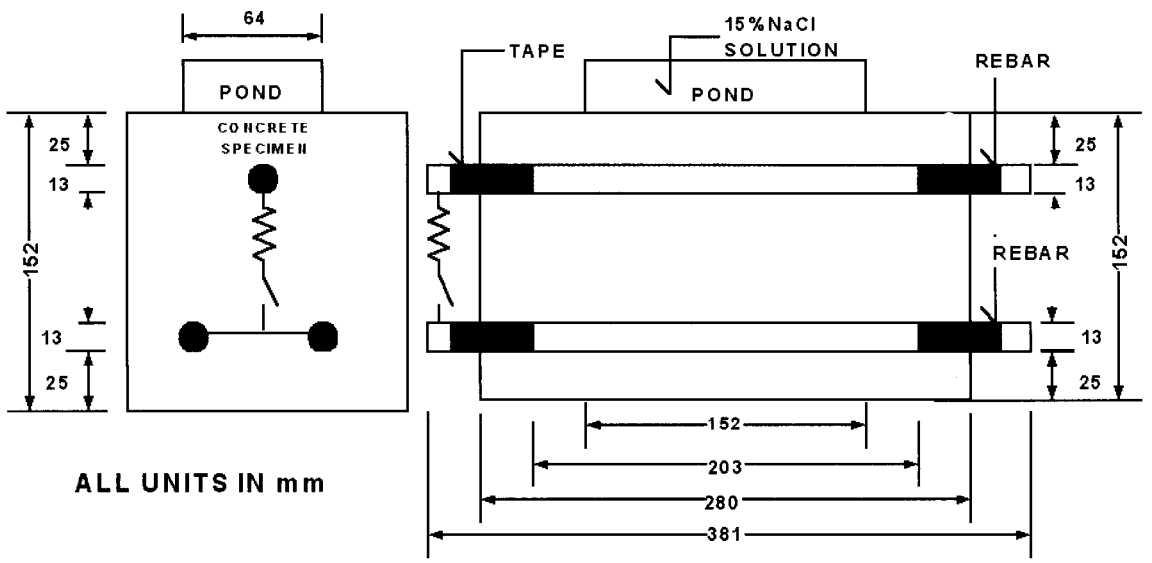

Fig. 1. Geometry of the classical G109 specimen

tinued for nearly 5 years(1800 days) using a 15 w/o NaCl solution. At the end of the dry cycle, potential and macro-cell current data were acquired from each specimen. Macro-cell current between the top and two bottom bars was measured independently from the voltage drop across the shunt and by a zero resistance ammeter with the shunt by-passed. Corrosion was defined as having initiated when the macro-cell current was 10 μA or greater and the potential for the top bar was - 0.28 V_{SCE} or more negative for two consecutive data acquisition periods. Later, this definition was relaxed; and active corrosion was defined solely in terms of potential having decreased to -0.28 V_{SCE}. When a specimen became active, it was autopsied; and the corrosion state was assessed. In addition, a powder drilling was acquired along the upper portion of the top rebar trace at both the corrosion site and elsewhere where the steel had remained passive for chloride analysis. These analyses were performed using the FDOT(Florida Department of Transportation) acid soluble method.[11]

3. Results and discussion

3.1 Corrosion features of mixes

During the 1800 days of test period, 24 of the 36 reinforced G109 specimens had actively corroded. Table 3 provides a listing of all specimens and of the T_i value in the case of corrosion activity. In instances where T_i was relatively brief, the shift in corrosion potential from the range indicative of passivity to that of active corrosion was relatively abrupt. Concurrently, macro-cell current increased from negligible to greater than 10 μA. In the case of specimens that became active after relatively long exposure, this change was more gradual and potential and current density sometimes reverted to values indicative of the passive state.

Fig. 2 presents a current versus time plot for specimens of the low alkalinity and high w/c mix design (LA0.50), which exemplifies the former type of behavior. Specimens of this type became active relatively early because of comparatively low concrete resistivity, as affected by the high w/c, and corrosion was typically pronounced. Correspondingly, Fig. 3 presents comparable data for specimens that became active after relatively long exposure times (HA0.4). In these cases, corrosion, once initiated, was relatively modest due to the beneficial effects of the lower w/c and inhibiting nature of the high alkalinity cement.

For specimens in the second category, corrosion was considered to have initiated at the time when potential first became more negative than -0.28 V_{SCE}, irrespective of any subsequent, more positive potential drift. Macro-cell current was often less that 10 μA at this time. All speci-

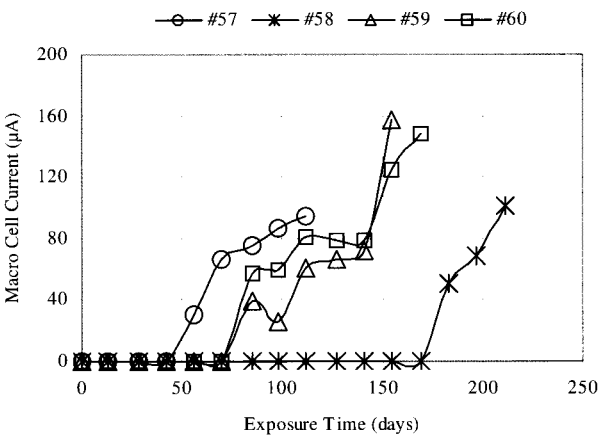

Fig. 2. The current change of LA0.50 type specimens.

Table 3. Specimen configurations and list of time to corrosion (Ti).

Specimen No.	Mix Design	T_i (Days)	Specimen No.	Mix Design	T_i (Days)	Specimen No.	Mix Design	T_i (Days)
1	HA0.37	>1800	22	NA0.37	>1800	43	LA0.37	>1800
2	HA0.37	>1800	23	NA0.37	>1800	44	LA0.37	>1800
3	HA0.37	>1800	24	NA0.37	1096	45	LA0.37	190
4	HA0.37	>1800	25	NA0.37	1192	46	LA0.37	>1800
8	HA0.41	>1800	29	NA0.41	136	50	LA0.41	297
9	HA0.41	1329	30	NA0.41	206	51	LA0.41	>1800
10	HA0.41	1192	31	NA0.41	339	52	LA0.41	567
11	HA0.41	1401	32	NA0.41	1120	53	LA0.41	>1800
15	HA0.50	136	36	NA0.50	93	57	LA0.50	107
16	HA0.50	306	37	NA0.50	93	58	LA0.50	234
17	HA0.50	297	38	NA0.50	136	59	LA0.50	136
18	HA0.50	225	39	NA0.50	178	60	LA0.50	136

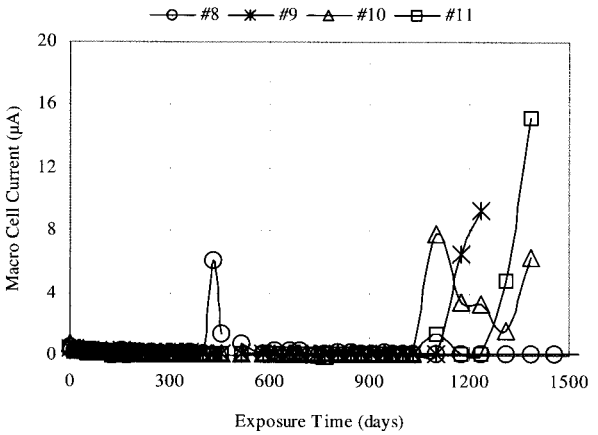

Fig. 3. The current change of HA0.41 type specimens.

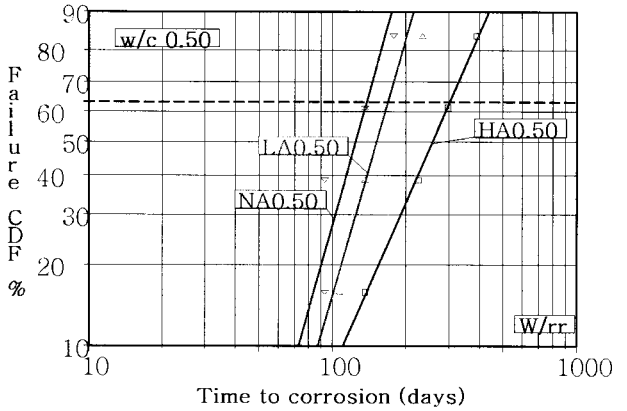

Fig. 4. The Weibull plot for w/c 0.50.

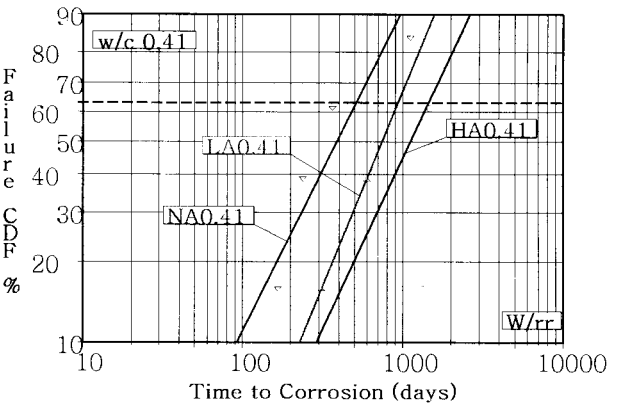

Fig. 5. The Weibull plot for w/c 0.41.

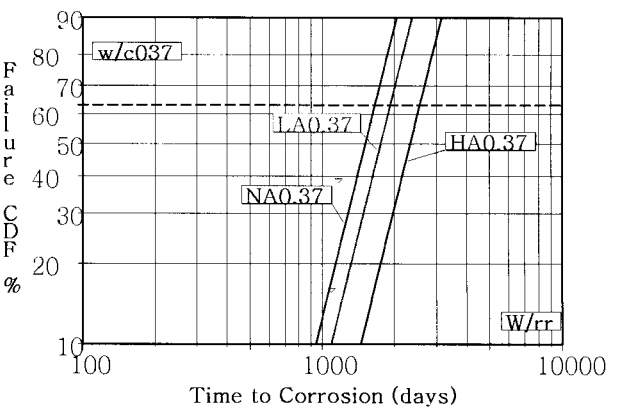

Fig. 6. The Weibull plot for w/c 0.37.

mens that met the criteria for having initiated corrosion, either the original or relaxed, were sectioned and examined; and active corrosion was confirmed in all cases, although attack was less advanced for the latter compared to the former.

3.2 Time-to-corrosion

Weibull analysis is a commonly employed engineering and scientific tool for representing and projecting failures. The two-parameter Weibull distribution is described by the expression,

$$F(T) = 1 - e^{(\frac{T}{\eta})^{\beta}} \quad (2)$$

where, F(T) is the cumulative distribution function (CDF) of the corroded fraction, T is failure time (T_i), η is scale parameter, and β is slope or shape parameter. Here, η is the characteristic life or the time at which 63.2 percent of the population failed. The value for β can infer mechanistic information.[12),13)] Thus, $\beta < 1$ indicates early-age failures, as can occur as a consequence of manufacturing defects. Situations where $\beta = 1$ constitute random failures, whereas failures with $\beta > 1$ are indicative of wear out.

Accordingly, Figs. 4~6 show CDF verse Ti plots for each of the three cement alkalinities and w/c 0.50, 0.41 and 0.37, respectively. Clearly, the lack of active specimens in the case of w/c 0.37 precludes interpretation here other than to affirm the beneficial effect of low w/c. In some cases where relatively few specimens have initiated corrosion, β was forced using a value that was judged appropriately based upon the behavior of other specimens of the same w/c.

Fig. 7 shows the overall trend of η with respect to w/c and cement alkalinity. These results indicate that, first, η increased with decreasing w/c, and, second, η was highest for the HA specimens. However, a generalized trend of increasing η with increasing cement alkalinity was not disclosed, since η was greater for the LA than for the NA for each w/c. Again, caution must be needed with

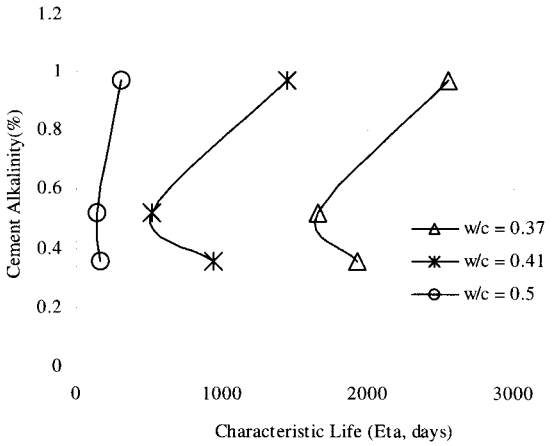

Fig. 7. The overall trends of Characteristic Life Eta (η).

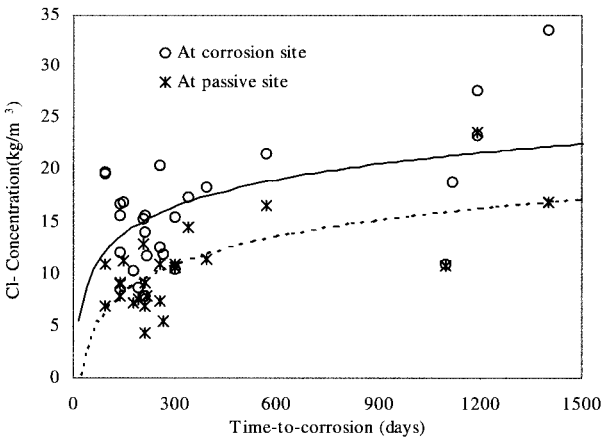

Fig. 8. Chloride thresholds (Cl^-_{th}) with respect to time-to-corrosion (T_i).

regard to interpretation because of the small number of specimens; however, based upon these results, T_i for the HA specimens exceeded that for the NA and LA by a factor or 1.7~5.1. The finding that Eta (η) for the LA mix design specimens exceeded that of the NA ones may relate to reduced Cl^- binding with increasing OH^- over the pH range that applies here.[14]

3.3 Chloride analysis

Table 4 lists [Cl^-] values that were measured for powdered concrete samples acquired along the upper rebar trace, both at the active corrosion site and elsewhere where the steel remained passive. Also listed are T_i and the exposure time at which active specimens were autopsied. From these times and the D_{eff} (effective diffusion coefficient) values, [Cl^-] at time T_i was back calculated; and this calculated value was taken as Cl^-_{th}.

Fig. 8 shows a plot of Cl^-_{th} versus T_i and indicates that in most cases [Cl^-] at the active corrosion site exceeded that of passive site. However, not in all but one of the cases where specimen autopsy was performed at the time when potential first became negative to -0.28 V_{SCE}, and [Cl^-] at the active and passive sites was approximately the same. This suggests that the elevated [Cl^-] at the corrosion site resulted from electro migration subsequent to corrosion initiation. Therefore, [Cl^-] at the passive sites was considered as chloride threshold value (Cl^-_{th}). The general trend in Fig. 8 is one where Cl^-_{th} increased with time irrespective of mix designs. This is consistent with; first, chlorides having been continued to progressively accumulate with increasing time and, second, T_i being a statistically distributed parameter.

Fig. 9 presents Cl^-_{th} versus cement alkalinities(M[OH-],

Table 4. Chloride concentration data at corrosion site and place that remain passive state.

Specimen No.	[Cl^-] Active	[Cl^-] Passive	Time to corrosion	Expo. time	Specimen No.	[Cl^-] Active	[Cl^-] Passive	Time to corrosion	Expo. time
10-HA0.41	23.27	23.53	1192	1459	32-NA0.41	18.76	-	1120	1186
11-HA0.41	33.50	16.82	1401	1455	36-NA0.50	19.67	10.93	93	183
15-HA0.50	11.98	8.92	136	211	37-NA0.50	19.56	6.90	93	213
16-HA0.50	15.39	10.59	306	324	38-NA0.50	16.62	9.13	136	256
17-HA0.50	18.28	11.32	297	433	39-NA0.50	10.22	7.29	178	211
18-HA0.50	12.54	10.92	225	319	45-LA0.37	16.90	11.22	190	211
24-NA0.37	10.93	10.76	1096	1124	50-LA0.41	10.44	10.95	297	324
25-NA0.37	27.64	-	1192	1229	52-LA0.41	21.46	16.49	567	576
29-NA0.41	15.63	7.92	136	211	58-LA0.50	11.87	5.42	234	264
30-NA0.41	15.81	12.86	206	256	59-LA0.50	15.61	4.31	136	211
31-NA0.41	17.39	14.41	339	381	60-LA0.50	20.33	7.37	136	190

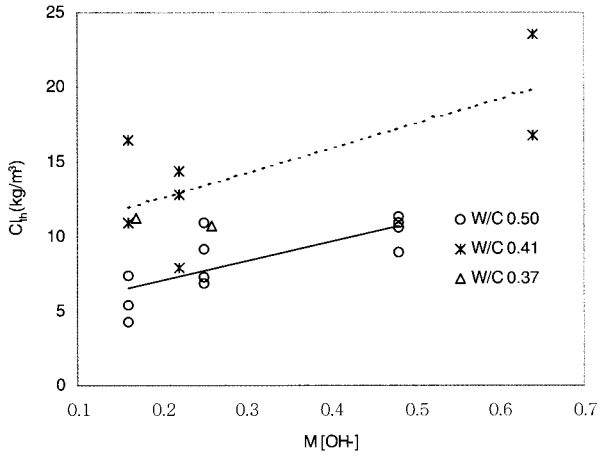

Fig. 9. The change of chloride thresholds (Cl^-_{th}) with respect to $M[OH^-]$.

molality of hydroxyl ion) plot and this result indicated that the higher cement alkalinity elevated the chloride threshold levels irrespective of T_i. Also, the improved time-to-corrosion for HA type specimens compare to type LA and NA can be explained by this elevated Cl^-_{th}.

Generally, values for Cl^-_{th} in the range 0.60-0.75 kg/m^3 have historically been reported[15),16)] and are widely referenced in North America concrete studies. Also, the upper limit of Cl^-_{th} values[17)] reported by Glass and Buenfeld (9.7 kg/m^3; concrete weight basis for the cement content of the present specimens) approximates the mid-value determined from the present research. The possible reasons of high Cl^-_{th} in this study can be 1) relatively constant relative humidity and temperature exposure condition, 2) polished rebar surface condition, 3) relatively small size of specimen, etc. To find better idea on the revealed high Cl^-_{th} compare to historical values, however, the more investigations are needed.

4. Conclusions

The following conclusions were reached based upon exposure of a series of G109 specimens to cyclic wet and dry ponding with a 15 w/o NaCl solution.

1. Time-to-corrosion was a distributed parameter; and because of this, corrosion initiation for "four identical" specimens of each mix design varied, often over a relatively wide range.

2. Time for the onset of active corrosion, T_i, was least for ones that were of normal alkalinity (EqA 0.52), intermediate for a low alkalinity (EqA 0.36), and highest for high alkalinity (EqA 0.97) cement. Time-to-corrosion did not increase monotonically with cement alkalinity, however, presumably as a consequence of relatively high Cl^- binding in the lower pore water pH range.

3. The chloride threshold level, Cl_{th}, increased with increasing T_i and cement alkalinity. Consequently, the HA specimens exhibited the highest Cl_{th} compare to LA and NA at the same w/c. Local chloride concentrations along the rebar trace varied from active to passive site. This difference presumably resulted from electro-migration of Cl^- to active sites subsequent to corrosion initiation. Therefore, Cl at passive site was considered to represent chloride threshold values.

Thus, improved corrosion resistance and overall enhanced durability of concrete structures can be realized using cements of the HA type, provided alkali silica reaction is not a factor.

References

1. D. A. Hausmann, *Material Protection*, **6**(11), 19 (1967).
2. C. Alonso, C. Andrade, M. Castellote, and P. Castro, *Cement and Concrete Research*, **30**, 1047 (2000).
3. J. Nam, W. Hartt, K. Kim, and L. Li, NACE, Paper No. 03299, CORROSION/2003
4. L. O. Nilsson, E. Poulsen, P. Sandberg, H. E. Sörensen, and O. Klinghoffer, "HETEK", The Road Directorate, Report No.53 (1996).
5. P. Longuet, L. Burglen, and A. Zelwer, *Rev. Matér.*, **35**, 676 (1973).
6. R. S. Barneyback and S. Diamond, *Cem. Concr. Res.*, **11**, 279 (1982).
7. C. L. Page and O. Vennesland, *Mater. Struct.*, **19**, 16 (1983).
8. A.A. Sagüés, E.I. Moreno, and C. Andrade, *Cement and Concrete Research*, **27**(11), 1747 (1997).
9. L. Li, A. A. Sagüés, and N. Poor, *Cement and Concrete Research*, **29**, Issue **3**, 315 (1999).
10. ASTM Standard Test Method G 109, 03.02 (1999).
11. "Florida Method of Test for Determining Low-Levels of Chloride in Concrete and Raw Materials," FM 5-516, FDOT (1994).
12. T. Shibata, Corrosion Probability and Statistical Evaluation of Corrosion Data, in Uhlig's Corrosion Handbook, 2nd Ed., Ed: R. W. Revie, The Electrochemical Society, Pennington, NJ, p.367 (2000).
13. R. W. Staehle, NACE, Paper No. 02418, CORROSION/2002
14. P. Sandberg and J. Larsson, Chloride Penetration in Concrete Structures, Ed. L.-O Nilsson, Nordic Miniseminar, Göteborg, 98 (1993).
15. D. S. Spellman and R. F. Stratfull., Highway Research Record, No.423, 27 (1963).
16. K. C. Clear, Report No. FHWA-RD-76-70, Federal Highway Administration (1976).
17. G. K. Glass and N. R. Buenfeld, paper no. 3, RILEM International Workshop on Chloride Penetration into Concrete (1995).